Performance Investigation of IEEE 802.11af Systems Under Realistic Channel Conditions

Mustafa Can Macit,* Habib Şenol,† Serhat Erküçük*

*Department of Electrical-Electronics Engineering, Kadir Has University, 34083, Istanbul, Turkey
†Department of Computer Engineering, Kadir Has University, 34083, Istanbul, Turkey
Email: { mustafacan.macit, hsenol, serkucuk}@khas.edu.tr

***Abstract*—As the analog TV broadcasting channels have become less frequently used in the last decade, there has been a great interest in these frequency bands for the deployment of metropolitan, local and personal area networks. Among them, the local area network standard IEEE 802.11af defines PHY and MAC layer implementation of such networks in these unused frequency bands, also named television white space (TVWS). According to the standard, the systems may use contiguous or non-contiguous channels during their operation, depending on the channel availability. In this paper, we investigate in detail the performance of different operation modes of these systems under realistic channel conditions. While the perfect knowledge of channel would result in similar system performances, as the number of in-between-bands occupying the non-contiguous modes is increased the channel estimation performance degrades drastically, which is quantified in this study. In addition, it is shown that determining the true locations of multipaths heavily relies on the selected channel resolution and has a significant effect on the system performance. Numerical examples are given to demonstrate the effects of both the non-contiguous operation modes and the selected channel resolution.**

Keywords*—TV white space (TVWS), IEEE 802.11af, multi-channel operation modes, system performance, channel estimation

I. Introduction

Due to increasing demand for higher data rates and new wireless communication technologies, there has been a need for better utilization of the spectrum. In recent years, one important resource for new spectrum allocation has been the use of discontinued analog TV broadcasting bands, which are called the TV white space (TVWS). Considering the potential of using the TVWS for different applications, there have been standardization efforts for wireless regional, local and personal area networks. The systems designed based on these standards are seen as secondary systems and should not interfere with primary systems while they operate [1]. On the other hand, all these systems are based on independently operating networks, which should peacefully coexist with the other secondary network devices [2]. While coexistence of primary and secondary users, and coexistence among secondary users have been an important research area for both academia and industry, the U.S. regulatory agency Federal Communications Commission (FCC) has approved the opportunistic use of TVWS by TV band devices for improving spectrum efficiency [3]. This has allowed the companies to commercialize their products in the market while ensuring peaceful coexistence mechanisms.

Among Wireless Regional Area Network (WRAN), Wireless Local Area Network (WLAN) and Wireless Personal Area Network (WPAN) standardization activities, IEEE 802.11af standard defines the physical (PHY) and medium access control (MAC) layers for WLAN operation in TVWS [4]. Compared to other IEEE 802.11 based systems at 2.4 GHz and 5 GHz, the main advantages of the IEEE 802.11af systems are two-fold. First of all, IEEE 802.11af systems operate in the 470-710 MHz band. Hence, signal propagation characteristics at these frequencies are better compared to IEEE 802.11 systems at higher frequencies. Secondly, unused frequency bands (i.e., TV channels not active at that instant) can be used in order to increase the transmission bandwidth equivalent to or greater than the ones at 2.4 GHz and 5 GHz bands. This brings flexibility for operating with larger bandwidths.

Considering the advantages of a WLAN system in TVWS, the performance of IEEE 802.11af systems has been studied widely in the literature. In [5], the authors present the first ever prototype built based on the IEEE 802.11af standard considering both PHY and MAC layer aspects. The performance of PHY layer channel bounding is compared with MAC layer channel aggregation in terms of data rates and packet error rates in [6]. The performance of an IEEE 802.11af based network is analysed considering the effects of inter-access point interference and congestion in [7]. The performances of IEEE 802.11af, IEEE 802.22 and IEEE 802.15.4m are assessed while they are in close proximity, in order to determine tolerable interference levels in [8]. Packet error rate performances of IEEE 802.11af standard and the similar local area network standard ECMA-392 are compared considering the system parameters defined in the standards in [9]. In [10], a partial subcarrier system for the IEEE 802.11af systems is proposed to effectively use the TVWS and increase the throughput. While evaluating the system performances in [5]–[9], the simple operation mode of an IEEE 802.11af system that uses a single frequency band is considered. However, these systems may use multiple available channels, which may be contiguous or non-contiguous. In [10], the different operation modes are considered, however, the performances provided did not include the effects of channel estimation.

In this paper, motivated by investigating the effect of non-contiguous modes on the system performance, the performance of different operation modes of IEEE 802.11af systems is

978-1-4799-5344-8/15/$31.00 ©2015 IEEE

studied in detail under realistic channel conditions. More specifically, the effect of channel estimation on the contiguous and non-contiguous operation modes is studied. While the perfect knowledge of channel would result in similar system performances, the degraded channel estimation performance is quantified as a function of in-between-bands occupying the non-contiguous mode. Furthermore, the effect of channel resolution for determining the true locations of multipaths for different channel resolutions is studied. Some numerical examples are given to demonstrate the effects of the non-contiguous operation mode and the selected channel resolution on the system performance.

The rest of the paper is organized as follows. In Section 2, contiguous and non-contiguous operation modes of IEEE 802.11af standard are explained. In Section 3, the system model that presents the IEEE 802.11af based signal model and the associated channel model is presented. In Section 4, a linear minimum mean-square error (LMMSE) based channel estimator that knows the multipath locations but estimates the tap coefficients is presented. In Section 5, simulation results are presented to demonstrate the effects non-contiguous operation modes and channel resolution on the system performance. Concluding remarks are given in Section 6.

II. IEEE 802.11AF OPERATION MODES

In order to achieve high data rates, TV High Throughput (TVHT) PHY has been defined in the standard [4]. Accordingly, the data transmission is based on orthogonal frequency division multiplexing (OFDM) systems, where the systems are named basic channel units (BCUs) having a bandwidth of 6 MHz, 7 MHz or 8 MHz, depending on the regulatory domain. Since the TVWS for the standard is considered as the 470-710 MHz bandwidth, for a BCU bandwidth of 6 MHz, there are 40 non-overlapping BCUs. While the IEEE 802.11af based devices have to support the mandatory transmission mode of one BCU (represented with TVHT-MODE-1), optional transmission modes use multi-BCUs and may achieve higher data rates.

There are four optional modes defined in the standard [4]:
1) Two contiguous BCUs (TVHT-MODE-2C)
2) Two non-contiguous BCUs (TVHT-MODE-2N)
3) Four contiguous BCUs (TVHT-MODE-4C)
4) Two non-contiguous frequency segments, each of which comprising two contiguous BCUs (TVHT-MODE-4N)

While an IEEE 802.11af based device may operate on contiguous BCUs (TVHT-MODE-2C and TVHT-MODE-4C) and increase its transmission bandwidth, depending on the unavailability of contiguous BCUs it may operate in the non-contiguous modes (TVHT-MODE-2N and TVHT-MODE-4N). Operation modes of two contiguous and non-contiguous BCUs are illustrated in Fig. 1. In the non-contiguous operation mode, the data subcarriers in the unused frequency bands can be nulled and the system complexity can be made comparable to the contiguous mode. Furthermore, under the perfectly estimated channel assumption, system performances can be found to be similar. However, in practice the frequency selective nature of the channel and the use of limited number of pilot tones[1] (6 for the mandatory mode) are expected to degrade the channel estimation performance as the separation between the non-contiguous BCUs is increased. This effect will be investigated considering the system design parameters defined in the standard and for practical channel models.

[1]Since the number of pilot tones is very low, a sparse multipath channel is assumed in order to decrease the unknown channel parameters to be estimated.

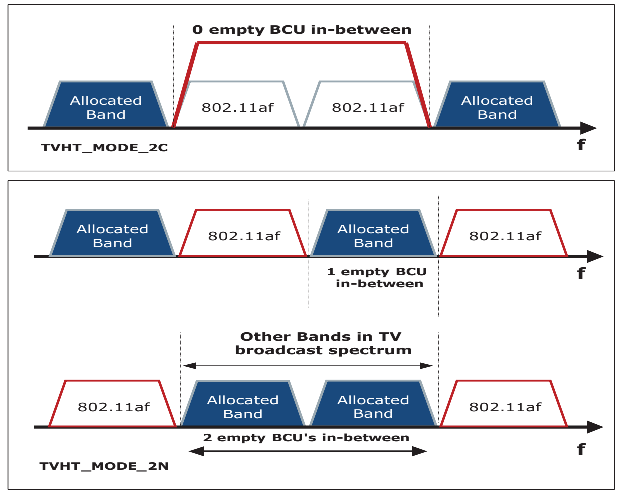

Fig. 1. Illustration of contiguous and non-contiguous operation modes

In the following, OFDM based IEEE 802.11af system and the channel model are explained.

III. SYSTEM MODEL

We consider a zero padded OFDM system with N subcarriers employing actively K subcarriers to transmit data symbols, and nothing is transmitted from the remaining $N-K$ carriers for the purpose of zero-padding. During any OFDM symbol, each active subcarrier is modulated by a data symbol $d_m[k]$, where m and k represent the OFDM symbol index and the discrete subcarrier frequency, respectively. After taking a K-point inverse fast Fourier transform (IFFT) of the data sequence and adding a cyclic prefix (CP) of duration T_{cp} before transmission to eliminate inter-symbol interference, the transmitted continuous time-domain complex valued signal can be expressed as

$$s(t) = \frac{1}{N}\sum_{m=0}^{M-1}\sum_{k=-K/2}^{K/2-1} d_m[k]\, e^{j2\pi k\,\Delta f (t-mT_{sym}-T_{cp})}\, \zeta(t-mT_{sym}), \quad (1)$$

where $\Delta f = 1/T$ is the OFDM subcarrier spacing, T stands for OFDM symbol duration, $T_{sym} = T + T_{cp}$ is the duration of an entire OFDM symbol, M is the OFDM block length, and $\zeta(t)$ denotes the unit pulse given by

$$\zeta(t) = \begin{cases} 1 & , \quad 0 \leq t \leq T_{sym} \\ 0 & , \quad \text{otherwise}. \end{cases} \quad (2)$$

The signal $s(t)$ is transmitted over a wireless multipath channel with impulse response given by

$$h(t) = \sum_{\ell=0}^{L-1} \alpha_\ell\, \delta(t-\tau_\ell)\ , \quad (3)$$

where L is the number of channel paths, $\delta(\cdot)$ stands for the Kronecker delta function, α_ℓ and τ_ℓ are the multipath gain and delay of the ℓth path, respectively. Independent path gains, $\{\alpha_\ell\}_{\ell=0}^{L-1}$, are zero-mean complex Gaussian random variables and have the normalized powers, $\{\Omega_\ell\}_{\ell=0}^{L-1}$, that obey an exponentially decaying power delay profile, $\Omega_\ell = Ce^{-\tau_\ell/T_{cp}}$, where C is the power normalization constant such that $\sum_{\ell=0}^{L-1}\Omega_\ell = 1$. The channel delays, $\{\tau_\ell\}_{\ell=0}^{L-1}$, are independent with respect to each other and uniformly distributed within the interval $[0, T_{cp}]$. Accordingly, the time domain received signal can be obtained as

$$
\begin{aligned}
y(t) &= \sum_{\ell=0}^{L-1} \alpha_\ell \, s(t-\tau_\ell) + w(t) \\
&= \frac{1}{N} \sum_{\ell=0}^{L-1} \sum_{m=0}^{M-1} \sum_{k=-K/2}^{K/2-1} \alpha_\ell \, d_m[k] \, e^{j\frac{2\pi k}{T}(t-\tau_\ell - mT_{sym} - T_{cp})} \\
&\quad \times \zeta(t-\tau_\ell - mT_{sym}) + w(t) \ , \qquad (4)
\end{aligned}
$$

where $w(t)$ is zero-mean complex additive white Gaussian noise (AWGN).

At the receiver, $y(t)$ is converted into the discrete-time signal by means of low-pass filtering and A/D conversion with the sampling interval $T_s = T/N$. Assuming that K active subcarriers are within the region of frequency response of both transmitter and receiver filters, and the number of channel paths and the path delays do not change during M OFDM symbol duration, it is sufficient to consider the channel estimation within M OFDM symbol block. Therefore, the nth time sample within mth OFDM symbol after the CP removal can be expressed as

$$
\begin{aligned}
y_m[n] &= y(mT_{sym} + T_{cp} + nT_s) \quad , \quad n = 0, 1, \cdots, (N-1) \\
&= \frac{1}{N} \sum_{\ell=0}^{L-1} \sum_{k=-K/2}^{K/2-1} \alpha_\ell \, d_m[k] \, e^{j\frac{2\pi k}{N}(n-\breve{\tau}_\ell)} + w_m[n] \ , \qquad (5)
\end{aligned}
$$

where $\breve{\tau}_\ell = \tau_\ell/T_s$ is the normalized delay of the ℓth path and $w_m[n] = w(mT_{sym} + T_{cp} + nT_s)$ denotes the AWGN sample at time n within mth OFDM symbol duration.

An $N-$point Fast Fourier Transform (FFT) is applied to transform the sequence $y_m[n]$ into frequency domain. The output at subcarrier k during mth OFDM symbol can be represented by

$$
\begin{aligned}
Y_m[k] &= \sum_{n=0}^{N-1} y_m[n] \, e^{-j\frac{2\pi}{N}nk} \ , \quad -\frac{K}{2} \le k \le \left(\frac{K}{2}-1\right) \\
&= \sum_{\ell=0}^{L-1} \alpha_\ell \, d_m[k] \, e^{-j\frac{2\pi k}{N}\breve{\tau}_\ell} + W_m[k] \ , \qquad (6)
\end{aligned}
$$

where $W_m[k] \sim \mathcal{CN}(0, N_0)$. It is straightforward that the vector form of (6) can be expressed as

$$
\mathbf{Y}_m = \sum_{\ell=0}^{L-1} \mathbf{a}_m(\breve{\tau}_\ell) \, \alpha_\ell + \mathbf{W}_m \ , \qquad (7)
$$

where

$$
\begin{aligned}
\mathbf{Y}_m &= \Big[Y_m\big[-\frac{K}{2}\big], Y_m\big[-\frac{K}{2}+1\big], \cdots, Y_m\big[\frac{K}{2}-1\big]\Big]^T \\
\mathbf{W}_m &= \Big[W_m\big[-\frac{K}{2}\big], W_m\big[-\frac{K}{2}+1\big], \cdots, W_m\big[\frac{K}{2}-1\big]\Big]^T \\
\mathbf{a}_m(\breve{\tau}_\ell) &= \mathbf{d}_m \odot \boldsymbol{\nu}(\breve{\tau}_\ell) \\
\mathbf{d}_m &= \Big[d_m\big[-\frac{K}{2}\big], d_m\big[-\frac{K}{2}+1\big], \cdots, d_m\big[\frac{K}{2}-1\big]\Big]^T, \qquad (8)
\end{aligned}
$$

$\boldsymbol{\nu}(\breve{\tau}_\ell)$ is a column vector with entries $e^{-j\frac{2\pi k}{N}\breve{\tau}_\ell}$, $(\cdot)^T$ denotes the transpose operator and $\odot$ stands for the Hadamard product. Stacking vectors in (7), we can rewrite the observation model as

$$
\mathbf{Y} = \sum_{\ell=0}^{L-1} \mathbf{a}(\breve{\tau}_\ell) \, \alpha_\ell + \mathbf{W} \ , \qquad (9)
$$

where

$$
\begin{aligned}
\mathbf{Y} &= \left[\mathbf{Y}_0^T, \mathbf{Y}_1^T, \cdots, \mathbf{Y}_{(M-1)}^T\right]^T \\
\mathbf{a}(\breve{\tau}_\ell) &= \left[\mathbf{a}_0^T(\breve{\tau}_\ell), \mathbf{a}_1^T(\breve{\tau}_\ell), \cdots, \mathbf{a}_{(M-1)}^T(\breve{\tau}_\ell)\right]^T \\
\mathbf{W} &= \left[\mathbf{W}_0^T, \mathbf{W}_1^T, \cdots, \mathbf{W}_{(M-1)}^T\right]^T, \qquad (10)
\end{aligned}
$$

In this work, we are mainly interested in estimation of sparse multipath channel based on the observation (9). The overall continuous-time channel impulse response is represented by a parametric model in which the ℓth distinct path is characterized by path delay, $\breve{\tau}_\ell$, and tap coefficient, α_ℓ. In practice, the sparsity assumption does not always hold due to the non-integer normalized path delays in the equivalent discrete-time baseband representation of the channel. Therefore, such an estimated channel may differ substantially from the original channel. To achieve a better channel estimation performance, the A/D conversion at the input of the OFDM receiver is implemented with a sampling period T_s/ρ, $\rho \in \{1, 2^1, 2^2, \cdots\}$ leading to a finer delay resolution. Consequently, the continuous-valued normalized path delays $\breve{\tau}_\ell, \ell \in \{0, 1, \cdots, (L-1)\}$ can be discretized as $\eta_\ell = \lfloor \frac{\tau_\ell}{T_s/\rho} \rfloor = \lfloor \rho \, \breve{\tau}_\ell \rfloor$ and take values from the set of possible discrete path delays

$$
\eta_\ell \in \{0, 1, \cdots, (\rho L_{cp} - 1)\}, \qquad (11)
$$

where $L_{cp} = \lfloor T_{cp}/T_s \rfloor$, and $\lfloor \cdot \rfloor$ denotes the floor operator. Based on the associated discrete random channel tap positions $\{\eta_\ell\}_{\ell=0}^{L-1}$, the received signal in (9) can be rewritten as

$$
\mathbf{Y} = \sum_{\ell=0}^{L-1} \mathbf{a}_{\eta_\ell} \, \alpha_\ell + \mathbf{W} = \mathbf{A}\widetilde{\boldsymbol{\alpha}} + \mathbf{W} \ , \qquad (12)
$$

where $\mathbf{a}_{\eta_\ell} = \mathbf{a}(\breve{\tau}_\ell)\big|_{\breve{\tau}_\ell = \eta_\ell/\rho}$ is the η_ℓth column vector of the so-called *dictionary matrix* $\mathbf{A} = [\mathbf{a}_0, \mathbf{a}_1, \cdots, \mathbf{a}_{(\rho L_{cp}-1)}] \in \mathcal{C}^{MK \times \rho L_{cp}}$. Vector $\widetilde{\boldsymbol{\alpha}}$ is the sparse multipath tap coefficient vector with unknown non-zero elements $\{\alpha_\ell\}_{\ell=0}^{L-1}$ at unknown tap positions, $\{\eta_\ell\}_{\ell=0}^{L-1}$. The estimation problem of non-zero elements of the sparse multipath tap coefficient vector $\widetilde{\boldsymbol{\alpha}}$ and tap positions in (12) can be solved by sparse signal recovery methods. For data detection, it is straightforward that the observation equation in (6) can be rewritten as

$$
Y_m[k] = H[k] \, d_m[k] + W_m[k], \qquad (13)
$$

where $H[k] = \sum_{\ell=0}^{L-1} \alpha_\ell \, e^{-j\frac{2\pi k}{\rho N}\eta_\ell}$ is the frequency domain channel response at discrete frequency k.

IV. Performance Under Partial Knowledge of Channel State Information

In this work, we are interested in performance investigation of different operation modes of *IEEE 802.11af* systems rather than solving the sparse channel estimation problem by sparse signal recovery methods [11], [12]. Assuming the partial knowledge of the channel state information (*i.e.*, known tap delay positions and unknown tap coefficients), we want to exhibit the performance comparisons for these operation modes. Under the assumption of known $\{\breve{\tau}_\ell\}_{\ell=0}^{L-1}$ for the perfect knowledge tap positions or known $\{\eta_\ell\}_{\ell=0}^{L-1}$ for the knowledge of tap positions at the nearest integer multiple of T_s/ρ, we employ the LMMSE estimator to estimate the nonsparse tap coefficient vector $\boldsymbol{\alpha} = [\alpha_0, \alpha_1, \cdots, \alpha_{(L-1)}]^T$. While applying the LMMSE estimator using (12), in order to obtain the dictionary matrix with column vectors $\{\mathbf{a}(\breve{\tau}_\ell)\}_{\ell=0}^{L-1}$ or $\{\mathbf{a}_{\eta_\ell}\}_{\ell=0}^{L-1}$ assuming perfect knowledge or the knowledge at the nearest integer multiple of T_s/ρ tap delay position, respectively, we use the pilot symbols in their respective positions and set the unknown data symbols to zero [11]. With the channel tap delay position knowledge, using the observation equation in (12), the LMMSE estimator of $\boldsymbol{\alpha}$ can be given as

$$\widehat{\boldsymbol{\alpha}} = \left(\mathbf{A}^{(p)\dagger}\mathbf{A}^{(p)} + N_0\,\boldsymbol{\Omega}^{-1}\right)^{-1}\mathbf{A}^{(p)\dagger}\mathbf{Y}^{(p)} \;, \tag{14}$$

where $(\cdot)^\dagger$ denotes the complex conjugate transpose operator, $\mathbf{Y}^{(p)}$ is the frequency domain receive vector having elements at pilot subcarriers and $\boldsymbol{\Omega}$ represents the diagonal covariance matrix of the nonsparse tap coefficient vector $\boldsymbol{\alpha}$. The covariance matrix $\boldsymbol{\Omega}$ has the main diagonal elements $\{\Omega_\ell\}_{\ell=0}^{L-1}$ that are determined with respect to tap delay positions. The dictionary matrix $\mathbf{A}^{(p)}$ can be obtained as $\mathbf{A}^{(p)} = [\mathbf{a}^{(p)}(\breve{\tau}_0), \mathbf{a}^{(p)}(\breve{\tau}_1), \cdots, \mathbf{a}^{(p)}(\breve{\tau}_{(L-1)})]$ or $\mathbf{A}^{(p)} = [\mathbf{a}^{(p)}_{\eta_0}, \mathbf{a}^{(p)}_{\eta_1}, \cdots, \mathbf{a}^{(p)}_{\eta_{(L-1)}}]$ while assuming perfect knowledge or the knowledge at the nearest integer multiple of T_s/ρ tap delay position, respectively.

After obtaining the LMMSE estimate of the tap coefficient vector, $\widehat{\boldsymbol{\alpha}}$, using (13), the soft data symbols can be recovered by the LMMSE equalizer as follows

$$\widehat{d_m}[k] = \frac{\widehat{H}^*[k]}{\left|\widehat{H}[k]\right|^2 + N_0}\,Y_m[k] \;, \tag{15}$$

where $(\cdot)^*$ denotes the complex conjugate operator and $\widehat{H}[k]$ is the estimate of the channel response at subcarrier k that is determined as $\widehat{H}[k] = \sum_{\ell=0}^{L-1}\hat{\alpha}_\ell\, e^{-j\,\frac{2\pi k}{N}\breve{\tau}_\ell}$ or $\widehat{H}[k] = \sum_{\ell=0}^{L-1}\hat{\alpha}_\ell\, e^{-j\,\frac{2\pi k}{\rho N}\eta_\ell}$ for perfect knowledge or the knowledge at the nearest integer multiple of T_s/ρ tap delay position, respectively.

However, since $d_m[k]$ is discrete, belonging to a signal constellation point, we must quantize $\widehat{d_m}[k]$ to its nearest constellation point.

V. Simulation Results

In this section, symbol-error rate (SER) performances of the contiguous mode TVHT-MODE-2C and the non-contiguous mode TVHT-MODE-2N are studied. Specifically, the effects of (i) number of channel paths, (ii) channel resolution and (iii) the separation between OFDM symbols are investigated. The simulation parameters for both operation modes are given in Table-I and are consistent with the system parameters provided in [4]. Note that the OFDM block length, $M = 2$, refers to the mode TVHT-MODE-2C with no empty BCUs in-between the OFDM symbols, whereas $M \in \{4, 6, 8\}$ refers to the mode TVHT-MODE-2N with $\{2, 4, 6\}$ empty BCUs, respectively, in-between the OFDM symbols.

TABLE I. Simulation parameters for the contiguous mode TVHT-MODE-2C and the non-contiguous mode TVHT-MODE-2N

Constellation type	QPSK, 16QAM
OFDM block length (M)	$\{2, 4, 6, 8\}$
Number of empty BCU's ($M-2$)	$\{0, 2, 4, 6\}$
Channel bandwidth per OFDM symbol (BW)	6 MHz
Number of subcarriers per OFDM symbol (N)	144
Number of active subcarriers per OFDM symbol (K)	128
Subcarrier spacing (Δf)	$41\frac{2}{3}$ KHz
Guard interval rate	$\frac{1}{8}$
Number of pilot data per OFDM symbol	6

In Fig. 2, the effect of number of channel paths is investigated for TVHT-MODE-2C when QPSK modulation is used. It is assumed that the tap coefficients are perfectly known and the tap delay positions are discretized to the nearest integer multiple of T_s/ρ tap delay position when $\rho = 4$. Independent of the number of paths, knowing the delay positions perfectly serves as a benchmark. When $L = 1$, there is a slight degradation with respect to the ideal case. However, as L increases the SER performance degrades significantly. This is due to not accurately estimating the exact path locations for a given discrete channel resolution. Hence, the effect of channel resolution should be studied for a given number of channel paths.

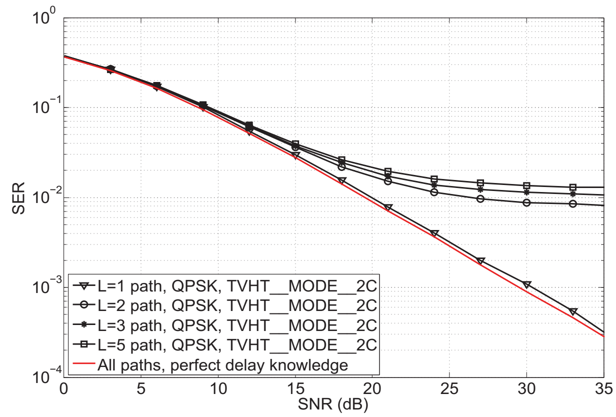

Fig. 2. SER performance of TVHT-MODE-2C for different number of channel paths

In Fig. 3, the effect of channel resolution is investigated for TVHT-MODE-2C when QPSK modulation is used and $L = 3$ is selected. For both known and estimated channel tap coefficients, the SER performance is studied when the delays are perfectly known and the resolution factor is chosen as $\rho \in \{1, 4, 8\}$. For the same channel resolution, estimating the tap coefficients is only about 0.5-1 dB inferior to perfect knowledge of the tap coefficients in the medium and high signal-to-noise-ratio (SNR) regions. On the other hand, it can be observed that

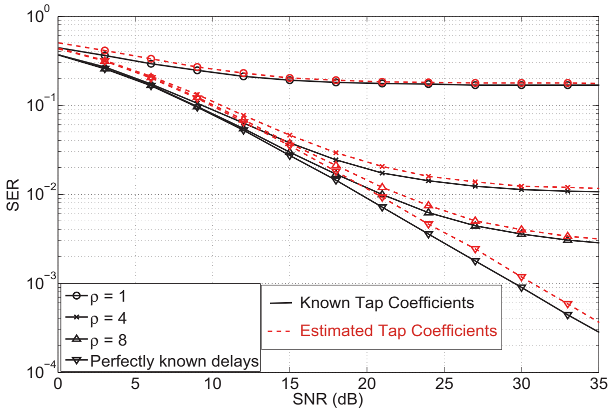

Fig. 3. SER performance of TVHT-MODE-2C for different channel resolutions

the selected channel resolution significantly affects the channel estimation, hence, the SER performance. By increasing the channel resolution, the perfectly known delay performance can be approached. It should be noted that appropriate sparse signal recovery methods are necessary for practical implementation.

In Fig. 4, performances of TVHT-MODE-2C and TVHT-MODE-2N are compared for different number of in-between empty BCUs for QPSK and 16QAM modulations. For fairness

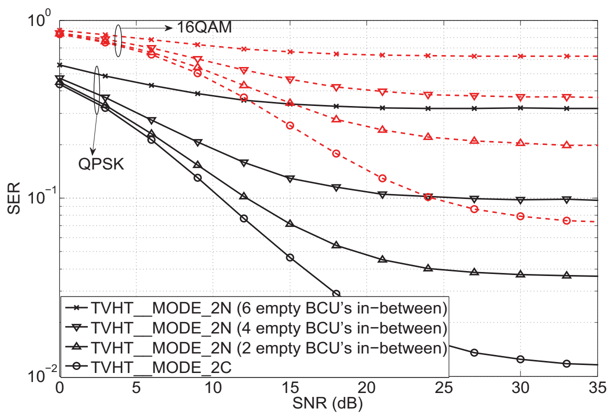

Fig. 4. SER performance comparison of TVHT-MODE-2C and TVHT-MODE-2N for different number of in-between empty BCUs

to all modes, the channel resolutions have been fixed to $\rho = 4$, and both channel tap delay positions and coefficients are estimated. It can be observed that as the number of in-between empty BCUs increases, the SER performance degrades. This is due to the interpolation error of channel estimation increasing as the separation between two OFDM symbols is increased.

While this study assumed the partial knowledge of the channel state information, future work will include the derivation of a mean-square error (MSE) lower bound of sparse channel estimation for IEEE 802.11af systems.

VI. Conclusion

In this paper, the practical implementation of the WLAN standard IEEE 802.11af is considered under realistic channel conditions. Since the number of pilot tones allowed in the standard is very low, a sparse multipath channel model is used in order to decrease the unknown channel parameters resulting in a better channel estimation performance. In order to increase the transmission bandwidth, the standard allows the use of non-contiguous BCUs. This separation between OFDM symbols and a low resolution of the discrete equivalent multipath channel may have negative effects on the overall system performance. In this study, the effects of channel resolution and the separation between BCUs in non-contiguous mode were investigated for the IEEE 802.11af systems under various practical scenarios. As the number of in-between-bands occupying the non-contiguous modes was increased the channel estimation performance degraded drastically. In addition, it is shown that determining the true locations of multipaths heavily relied on the selected channel resolution and has a significant effect on the system performance. Numerical examples were given to demonstrate the effects of both the non-contiguous operation modes and the selected channel resolution.

Acknowledgment

This research has been supported in part by Türk Telekom and Argela under the TT Collaborative Research Awards programme.

References

[1] C.H. Sun, G.P. Villardi, Z. Lan, Y.D. Alemseged, H.N. Tran, and H. Harada, "Coexistence of secondary user networks under primary user constraints in TV white space," *Proc. IEEE WCNC*, pp. 2146–2150, Apr. 2012.

[2] T. Baykas, M. Kasslin, M. Cummings, H. Kang, J. Kwak, R. Paine, A. Reznik, R. Saeed, and S.J. Shellhammer, "Developing a standard for TV white space coexistence: technical challenges and solution approaches," *IEEE Wireless Commun.*, vol. 19, pp. 10-22, Feb. 2012.

[3] Federal Communications Commission, Third Memorandum and Order, Apr. 2012.

[4] IEEE Std 802.11af, IEEE Standard for information technology – Telecommunications and information exchange between systems - Local and metropolitan area networks - Specific requirements - Part 11: Wireless LAN Medium Access Control (MAC) and Physical Layer (PHY) Specifications Amendment 5: Television White Spaces (TVWS) Operation, 2013.

[5] Z. Lan, K. Mizutani, G. Villardi, and H. Harada, "Design and implementation of a Wi-Fi prototype system in TVWS based on IEEE 802.11af," *Proc. IEEE WCNC*, pp. 750–755, Apr. 2013.

[6] Z. Lin, M. Ghosh, and A. Demir, "A comparison of MAC aggregation vs. PHY bonding for WLANs in TV white spaces," *Proc. IEEE PIMRC*, pp. 1829–1834, Sep. 2013.

[7] L. Simic, M. Petrova, and P. Mahonen, "Wi-Fi, but not on steroids: performance analysis of a Wi-Fi like network operating in TVWS under realistic conditions," *Proc. IEEE ICC*, pp. 1533–1538, Jun. 2012.

[8] C.-S. Sum, M.-T. Zhou, L. Lu, F. Kojima, and H. Harada, "Performance and coexistence analysis of multiple IEEE 802 WPAN/WLAN/WRAN systems operating in TV white space," *Proc. IEEE DySPAN*, pp. 145–148, Apr. 2014.

[9] J.-S. Um, S.-H. Hwang, and B.J. Jeong, "A comparison of PHY layer on the Ecma-392 and IEEE 802.11af standards," *Proc. ICST CROWNCOM*, pp. 315–319, Jun. 2012.

[10] K. Mizutani, Z. Lan, R. Funada, and H. Harada, "IEEE 802.11af with partial subcarier system for effective use of TV white spaces," *Proc. IEEE ICC*, pp. 1255–1259, Jun. 2013.

[11] C.R. Berger, S. Zhou, J. Preisig, and P. Willett, "Sparse channel estimation for multicarrier underwater acoustic communication: from subspace methods to compressed sensing," *IEEE Tran. Signal Process.*, vol. 58, pp. 1708–1721, Mar. 2010.

[12] Habib Senol, "Joint channel estimation and symbol detection for OFDM systems in rapidly time-varying sparse multipath channels," *Wireless Personal Communications*, DOI:10.1007/s11277-015-2273-x, Jan. 2015 (to be published).